AL-Bahir
Journal for Engineering and Pure Sciences
BJEPS

Manuscript 1109

Extraction of Mesoporous Silica from Local Soil Samples and Using as Sorbent in Dispersive Solid Phase Extraction Application

Zahraa Abdulsahib Qasim

Atheer Al Khudhair

Ahmed Fadhil Khudhair

ORIGINAL STUDY

Extraction of Mesoporous Silica From Local Soil Samples and Using as Sorbent in Dispersive Solid Phase Extraction Application

Zahraa A. Qasim, Atheer Al Khudhair, Ahmed F. Khudhair*

Department of Chemistry, College of Science, University of Kerbala, Karbala 56001, Iraq

Abstract

Mesoporous silica was successfully extracted from selected local soil samples (sandy, clay, and loamy) from Karbala city using sol-gel method. The extraction method was simple and environmentally friendly. Pure silica was characterized using different techniques such as EDX, SEM, BET, XRD, and FTIR. Amorphous silica was used as an adsorbent to extract Fe(III)-salicylicaldehyde oxime complex from aqueous solutions using solid phase extraction method. The optimum conditions of method were 0.10 gm of silica, 0.04 mol.L^{-1} of salicylaldehyde oxime reagent, pH 7.0, temperature 35 °C, shaking time 15 min, which showed very good extraction percent of Fe(III) - salicyaldehyde oxime complex 99.5 %. This indicates the success and selectivity of this method and its application to pharmaceutical samples containing iron (III) ions. It was concluded from this method that it is an easy,fast, low cost and high sensitively method.

Keywords: Amorphous silica, Sol-gel, Solid phase extraction, Water purification

1. Introduction

Amorphous Silica nanoparticles exhibit different physicochemical features like high specific surface area, large porosity [1], low toxicity, simple surface modification [2], adjustable mechanical, and physical characteristics [3]. Thus, SiO_2 nanoparticles were used in many applications related to water treatment systems (adsorbents), catalyst supports, drug delivery, agriculture, cosmetics [4], and sensors materials [5]. Various routes have been developed for obtaining silica such as sol-gel, aggregation,stöber method [6], emulsion and precipitation [7]. Sol-gel route is one of the most alternative and simplest routes for developing nanoparticles since it produces highly pure nanoparticles at mild temperatures [8]. It has various advantages over alternative synthesis routes including simple, less expensive, good control of texture, high quality, and high specific surface area of materials [9]. Sol-gel based silica materials may go back to 1640 when van Helmont first identified "water glass" through silicate dissolution under alkali conditions followed by acidified, silica gel precipitates [10]. Silica nanomaterial derived from natural resources like sand and rice husk has attracted extensive interest in different fields due to its affordable and environmentally friendly synthesis process [11,12], and used as efficient adsorbing material for separation of metals from solid-phase extraction (SPE) [13]. Silica is an ideal support for organic groups because it is a stable under acidic conditions and non-swelling inorganic material, and has high mass exchange characteristics and very high thermal resistance [14]. It was used to adsorbent Fe (III)- salicylaldehyde oxime complex from aqueous solutions [15]. While Dispersive solid-phase extraction is a variant of solid-phase extraction to extract efficiency of specific compounds from complex mixtures [16,17]. Substance powder was added to a liquid sample and stirred, the amount of analyte deposited on the

Received 7 May 2025; revised 4 June 2025; accepted 11 June 2025.
Available online 23 September 2025

* Corresponding author.
E-mail address: ahmmed.mutar@uokerbala.edu.iq (A.F. Khudhair).

https://doi.org/10.55810/2313-0083.1109

surface of the sorbent particles dispersed in the maximum value of solution reaches [18]. The liquid sorption is then separated from the sorbent. That Dispersive solid-phase extraction (DSPE) has several advantages are used of solvents significantly reduced, not require constant supervision, and no need for any fixed [19].

The study aimed to extract mesoporous silica from different types of local soil samples from Karbala city and used as adsorbent material to extract the Iron (III) salicylaldehyde oxime complex from aqueous solutions by dispersive solid phase extraction method.

2. Sampling

Samples were collected from several soils in the west and northeast from Karbala city from Iraq. The first sample is sandy soil. It is located in the desert area west of Karbala, near Lake Razzaza. The second and third samples are clay soils located near the Al Husseiniya River and the loamy soil is from orchards located in the Al Husseiniya district, northeast from Karbala city from Iraq as shown in Fig. 1.

3. Materials and method

Local soil, Hydrochloric acid (HCl 36 % Verdean House, New Delhi ＼India), Sodium hydroxide (NaOH 98 % SDFCL, Mumbai), Iron (III) chloride ($FeCl_3$ 99 % Ningbo Road, China), Salicyaldehyde oxime ($C_7H_7NO_2$ 98 % Ltd Poole, England) and Distilled water. Whole chemicals were used as accepted without any purification.

3.1. Extraction silica from different types of soil samples method

Silica was extracted from local soil sample by using sol-gel method [20]. They were washed seven times with distilled water to remove adhering materials. They were then dried in an oven at 100 °C for 24 h and sieved using a 100-mesh sieve. 6.0 (gm) of samples were dissolved in 12 mL of 3 M HCl, and the solution were transferred into a reflux system with continuous stirring at 90 °C over night to separate other elements from the samples. Afterward, it was filtered, washed with distilled water to remove any remaining HCl and other salts, and then dried in an oven at 100 °C for 24 h. The sodium silicate was prepared from sodium hydroxide to purify silica in titration 1:7 weight ratio from pure silicate residue with sodium hydroxide in a and heated in a muffle furnace at 600 °C for 2 h using the alkali fusion method. After heating, the obtained dry sodium silicate (Na_2SiO_3) was diluted with distilled water and stirred on a hot plate at 250 rpm at 106 °C. followed by titration of the solution with 2 M HCl until the pH reached around 1–2 as tested with litmus paper and formation of a clean white gel of ($Si(OH)_4$). The silica gel was filtered using filter paper and washed multiple times with distilled water to remove NaCl from the solution. The resulting product was then dried in an oven at 80 °C for 24 h to obtain 3.4 gm of silica particles and stored in acoveered plastic container for later use to characterize by different techniques and using for diffrent applications.The samples are labeled S_1,S_2 and S_3 where S_1 is sandy soil, S_2 is clay soil and S_3 is loamy soil (see Scheme 1).

3.2. Iron (III) ion with salicylaldehyde oxime extract by solid phase (silica) method

Iron (III)- salicylaldehyde oxime complex was extracted by solid phase extraction method, it was dissolved (0.0343 gm) of iron (III) chloride in 100 mL of distilled water to prepare (1000) (mg. L^{-1}) of iron (III) solution. It was taking 2 mL of iron (III) solution was added to 2 mL of (0.01 mol. L^{-1}) of salicylaldehyde oxime to yield a dark violet of iron (III)-salicylaldehyde oxime complex with maximum absorption wavelength 520 nm as shown in Fig. 2. However, it was adjusted pH (2–11) with 0.1 mol. $L^{-1}$of HCl and NaOH. the salicylaldehyde oxime

Fig. 1. Different type of soil samples.

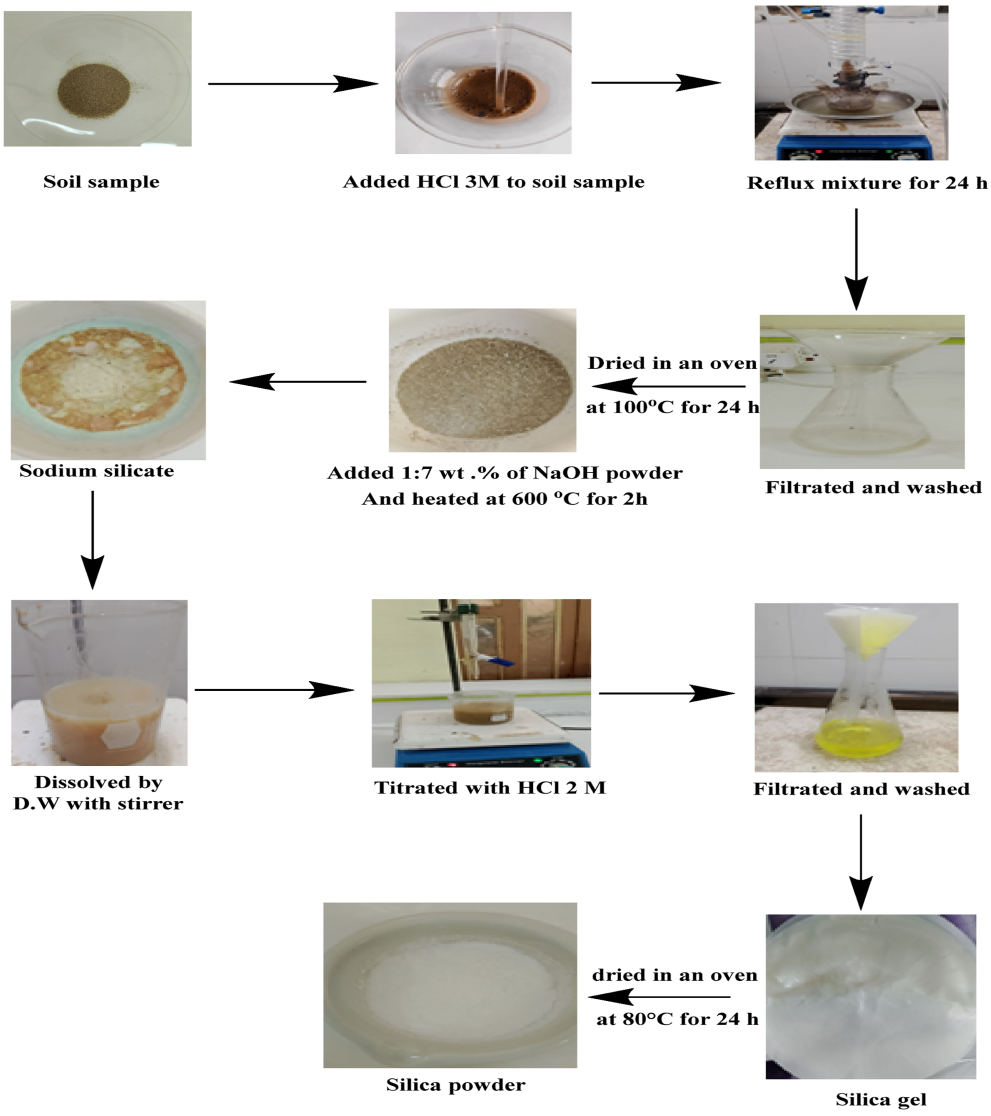

Scheme 1. Synthesized mesoporous silica from soil sample.

was taken in different concentration (0.01–0.05 mol. L^{-1}) under temperature (25–50 °C) as experimental condition. After that the iron (III) complex solution was added to prepare sorbent (silica) with different amounts (0.025–0125 gm). And Shaking the mixture with different time at 5–30 min, to allow the complex to adhere to the adsorbent (silica) as reaction equation in Fig. 2. After extraction residue solution was analyzed by using technique (Visible spectrophotometry) to confirm the extracted of the iron (III)- salicylaldehyde oxime complex by silica [21] (see Fig. 3).

4. Spectrophotometric determination of Fe (III) – Salicylaldehyde oxime complex

The calibration curve of Fe (III) - Salicyaldehyde oxime complex was constructed under optimum conditions at pH 7.0 and temperature 40°C. The absorbance was measured at 520 nm against Fe (III) - Salicyaldehyde oxime complex prepared in similar conditions. Fe (III) complex was indicated increasing the absorbance with increased concentration of Fe (III) complex in different ranges of concentration from 6 to 70 mg.L^{-1} at the linerty line as shown in Fig. 4, the calibration curve plotted between concentration of Fe (III) complex and absorbance [22].

5. Characterization

The obtained SiO_2 powder samples were characterized using different techniques. All powder samples were detected through X-ray diffraction (XRD) patterns and scanned from 10° to 80° of 2θ with Cu Kα radiation,manufacturer (Shimadizu X-

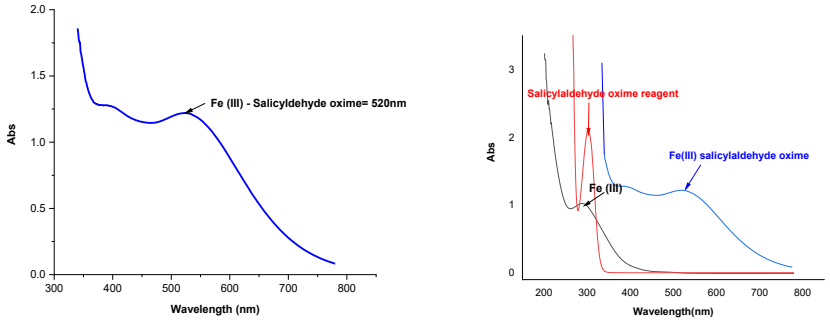

Fig. 2. Spectra of absorbtion for Fe (III) – Salicylaldehyde oxime solution and Fe (III) ion, Salicylaldehyde oxime reagent and Fe (III) – Salicylaldehyde oxime solution solution.

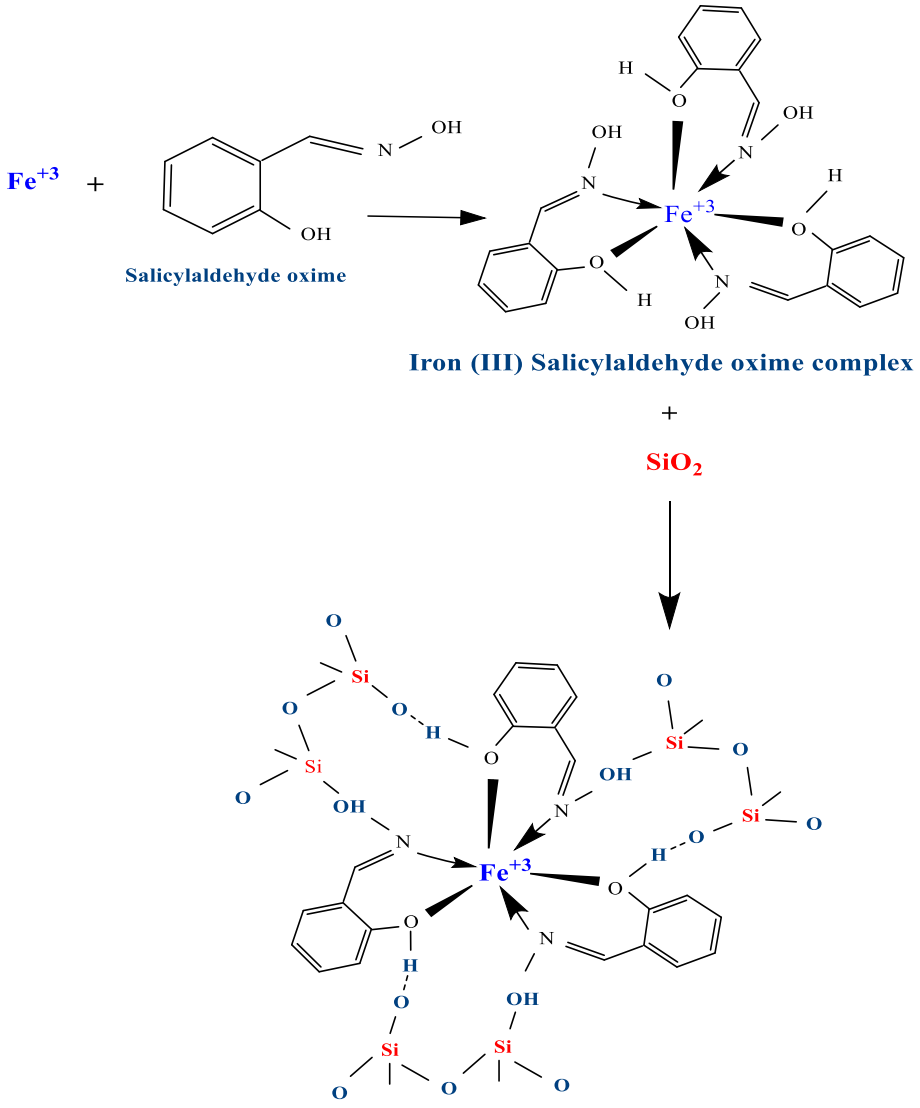

Fig. 3. Proposed reaction equation of Fe(III) – Salicylaldehyde oxime complex extraction by silica.

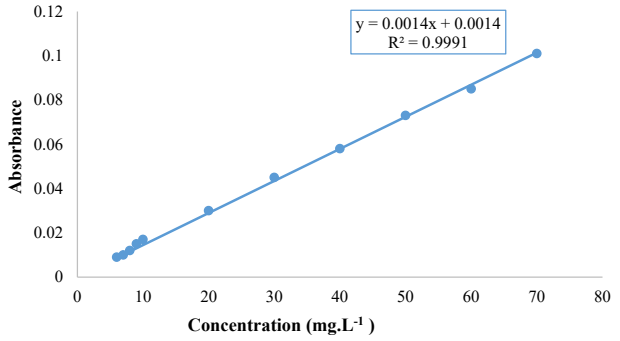

Fig. 4. Calibration curve of iron (III)- Salicyaldehyde oxime complex.

ray diffractometer) place of measurement (Beam Gostar Taban Lab＼ Iran) , Fourier transform Infrared (FTIR) measurement in the frequency range of 4000–400 cm^{-1} manufacturer (Shimadizu 8400s ＼ Japan), Scanning electron microscope (FESEM MIRA III (TESCAN): Beam Gostar Taban Lab＼ Iran) was used to analyze the surface morphology of samples. The surface area of samples was calculated by the BET equation using the N2 adsorption–desorption curves, measured in (BEL BELSORP MINI II: Beam Gostar Taban Lab＼ Iran). Scanning electron microscopy with an energy-dispersive X-ray (SEM ＼ EDX, AXIA CHEMI SEM Thermo scientific company: Hollande) was used to analyze the morphology and elemental compositions of the samples. The Atomic Forces microscopy (AFM) (CSPM-AA3000: Beam Gostar Taban Lab＼ Iran) used to determine particle size distribution, Ultraviolet–visible (UV–Vis) absorption spectra (MODEL UV – 1800 240 V: Japan), were recorded to using a UV–Vis diode array spectrometer for wavelength of iron complex. Visible spectrophotometer (model 721: Japan) at 520 nm was using to measure absorption of iron complex.

6. Result and discussion

In this study, **the Energy Dispersive X-ray (EDX) technique** was used to determine the percentage of elements in the three samples before and after extraction. As shown in Table (1), the weight values of the elements before and after extraction. As to silica percent, the results showed that sandy soil (S_1) contains the highest percentage of silica, and these results are consistent with the results of [23,24].

Scanning electron microscopy (SEM) has been used to make out the surface morphology, size and crystalline nature of silica sample produces by sol gel process. The morphology of silica particles was shown in Fig. 5(A,D), (B,E) and (C,F) images belong to S_1,S_2 and S_3 respectively. SEM images revealed that silica particles are highly agglomerated and spherical shaped and appear porous in nature. Where all images of different samples are similar.

The X-ray diffraction pattern (XRD) of SiO_2 samples are set out in (Fig. 6). The samples (S_1) and S_3 have exhibited high intensity peaks at around 20° [25] clay soil (S_2 (has shown low intensity [26]. Different sharp peaks appeared in S_2 sample at 32°, 48°, 58° ,78° belong to (Al_2O_3), MgO, CaO and Fe_2O_3 respectively [27–29]. Loamy soil (S_3) displayed small sharp peak at 48° of Fe_2O_3 [30].

2Fourier transform infrared spectroscopy (FTIR) analysis was used to determine functional groups of the samples on view in (Fig. 7). The vibrational strain of the Si-OH bond (silanol) in the amorphous SiO2 structure is indicated by the peak occurrence at wave 802.41 cm^{-1}. Furthermore, the O-Si-O (siloxy) bending vibrations are referenced by the peak at wave number 470.65 cm^{-1} and peak at 443.64 $cm^{-1}$to the bending vibrations of Si–O–Si groups [31], while the wave number at 960.58 cm^{-1} assigned to Si-O groups of the stretching vibration [32]. Moreover the bands at spectral regions between 3500 and 3300 cm^{-1} are characteristic for hydroxyl groups (O-H; stretching vibration) [33]. Finely the adsorption wave number at 1620 cm^{-1} to the O-H bending vibration [34]. These result are highly agree with EDX and XRD results.

Table 1. EDX analysis result of elements percentage in samples.

S_1			S_2		S_3	
Element Wt. (%)	Before Extraction	After Extraction	Before Extraction	After Extraction	Before Extraction	After Extraction
Si	34.4	31.8	13.0	13.4	15.2	12.5
O	53.9	50.8	48.3	49.4	50.2	50.1
C	7.00	8.50	11.1	27.4	12.1	10.6
Mg	1.00	0.00	3.50	0.50	3.20	0.00
Al	1.80	1.70	3.70	2.30	4.90	0.20
Ca	1.00	0.00	12.8	0.00	8.00	0.00
Fe	0.90	0.80	5.00	1.30	4.30	0.20

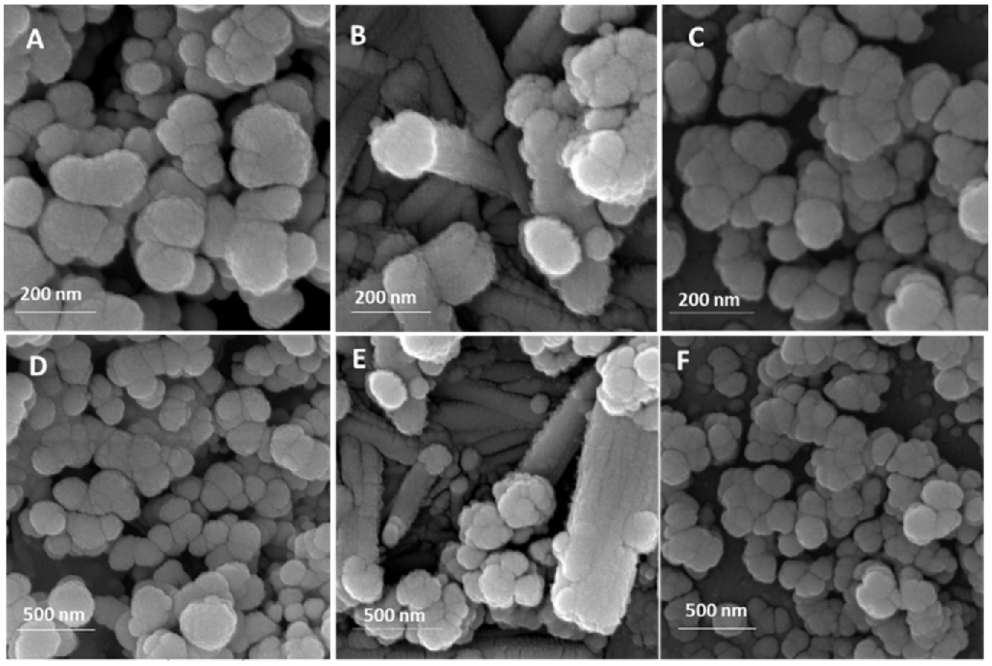

Fig. 5. SEM images of samples with different extracted silica: (A, D) S_1, (B, E) S_2, (C, F) S_3.

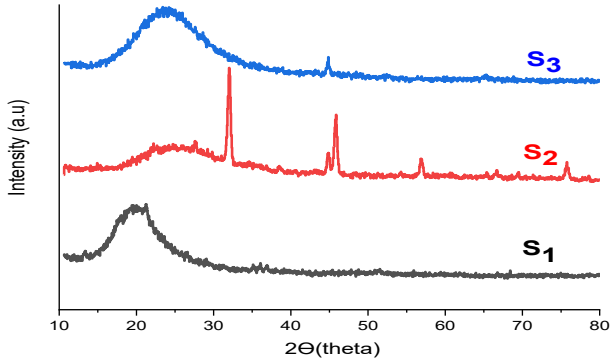

Fig. 6. XRD patterns of SiO_2 samples S1, S2 and S3.

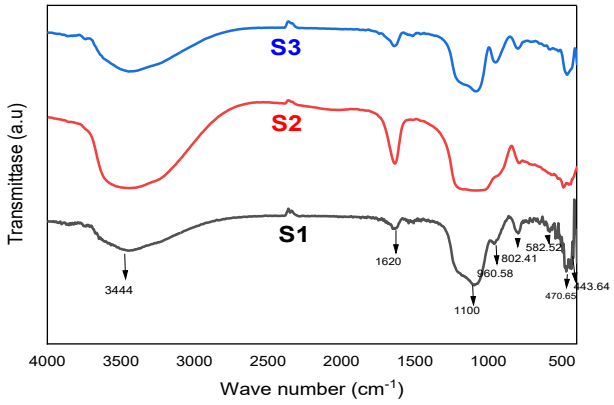

Fig. 7. FTIR spectrum of SiO_2 samples S_1,S_2 and S_3.

The specific surface areas, pores volume and pores size distribution data derived from nitrogen adsorption are shown in (Table 2). The sample S_1 showed higher specific surface area and pore volume than S_2 and S_3. [35]. Moreover, the pore dimeter was ranged from (11–13 nm), indicating that silica extracted are mainly mesoporous [36,37].

The adsorption desorption isotherms of nitrogen for the samples are recognized in (Fig. 8). The silica samples are indicating a type IV isotherm. That capillary condensation occurs and the pore exceeds a critical width. The pore size distribution is presented. That extracted silica indicates only mesoporous material [38].

7. Optimization of experimental condition of iron (III) extraction

Silica extracted from sandy soil was used as an adsorbent to extract iron (III) complex by solid phase extraction method under optimum conditions including: pH, concentration of reagent (salicylaldehyde oxime), amount of sorbent (silica), temperature equilibrium and shacking time. Which it used Fe^{3+} concentration:1000 $mg.L^{-1}$,

Table 2. Textural and structural properties of the extracted silica.

Samples	S_{BET} (m^2/g)	Vp (cm^3/g)	Dp (nm)
S_1	252.71	0.781500	11.207
S_2	12.767	0.047463	13.611
S_3	19.778	0.070416	13.023

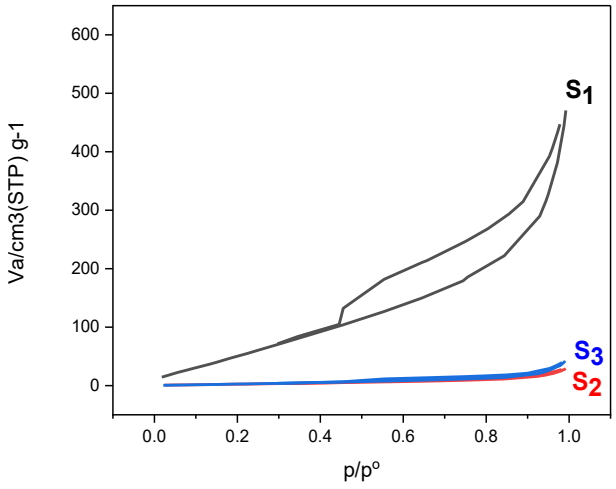

Fig. 8. Nitrogen adsorption-desorption isotherms of amorphous silica samples.

Concentration of salicylaldehyde oxime: (0.01–0.05) mol. L^{-1}, amount of sorbent (0.025–0.125) gm at different temperature (298–323) K and shacking time (5–30) min.

8. Influence of pH

It was most important influencing at the adsorption between iron complex and silica, the pH effect factor was studied in the range (2–11) that used 0.1 mol. L^{-1} from HCl and NaOH with using pH glass electrode to a justify pH. The results were shown in Fig. 9 and tabulated in Table S6 (https://bjeps.alkafeel.edu.iq/cgi/editor.cgi?article=1109&window=additional_files&context=journal) that obtained increasing adsorption of extracted complex with increase hydrogen ion function. Where best extraction percent at neutral medium pH 7, While basic medium was decreased for extraction percent of iron ligand complex due to the formation of complexes between iron and hydroxide ions [22].

9. Influence of salicylaldehyde oxime concentration

Under pH 7, the impact of the concentration (Conc.) of salicylaldehyde oxime reagent was using range concentration from 0.01 mol. L^{-1} to 0.05 mol. L^{-1}. It was increased the absorbance of iron complex with increasing concentration of reagent, and the best extraction the iron complex at 0.04 mol. L^{-1} as shown in Table S7 (https://bjeps.alkafeel.edu.iq/cgi/editor.cgi?article=1109&window=additional_files&context=journal) and Fig. 10 the effect concentration of salicylaldehyde oxime reagent to Fe (III) before and after adsorption.

10. Amount Sorbent effect

The effect of Amount Sorbent was used to adsorption iron (III) ligand complex under optimum condition at pH 7 and concentration salicylaldehyde oxime reagent 0.04 mol. L^{-1}. Which complex absorbance at 0.882. However, it was used different amounts sorbent of solid phase (silica) at (0.025–0.125) gm as shown in (Fig. 11) to extraction iron (III) ligand complex, And favorite amount sorbent to extraction iron (III) ligand complex at 0.1 gm.

11. Temperature effect

The influence of temperature on adsorption iron by silica was result investigated are shown in Table S8 (https://bjeps.alkafeel.edu.iq/cgi/editor.cgi?article=1109&window=additional_files&context=journal) and Fig. 12. The temperature was performed under optimum condition experimental at pH 7, concentration salicylaldehyde oxime

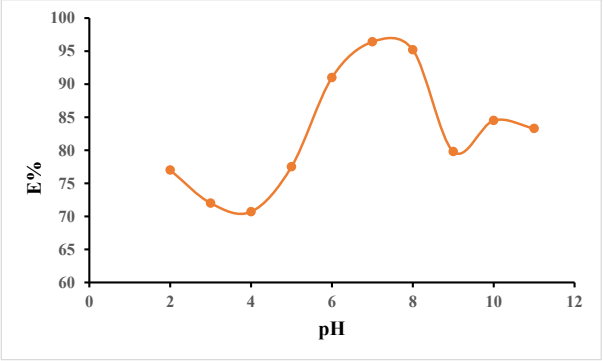

Fig. 9. Extraction percent of effect of pH solution on iron (III) complex adsorption on to SiO_2.

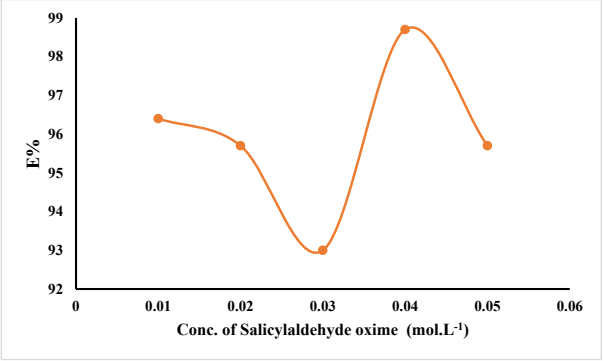

Fig. 10. Extraction percent agnist of concentration reagent (salicyaldehyde oxime) on iron (III) complex.

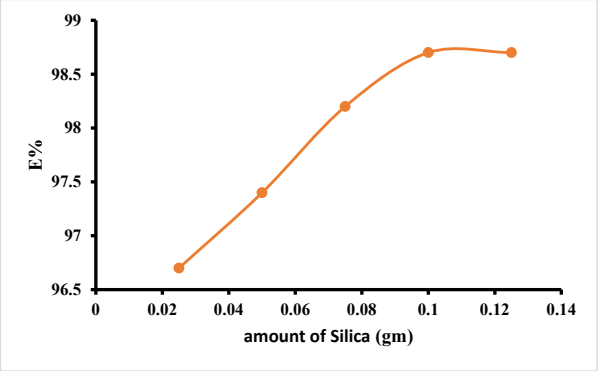

Fig. 11. Effect of different amount of sorbent (silica) on iron (III) complex.

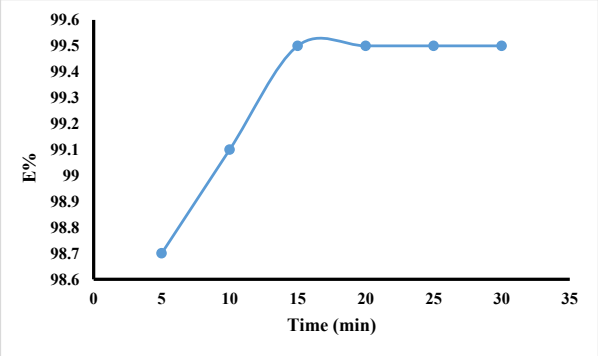

Fig. 13. Effect of time shacking on iron (III) complex adsorption on to silica.

reagent 0.04 mol.L^{-1} and amount sorbent 0.1 gm. The temperature effect are changing from 298 K to 323 K, while the temperature are most favorable at 308 K to removal iron, which the thermodynamic function (ΔHex,ΔGex,ΔSex) for collected result of these variables at (74.5, −41163, 133.9). The extraction process iron by using solid phase is an endothermic process with a positive value of an entropy indicates the formation electrostatic bonding of extracted ionic complex with silica [32]. The reaction is chemical Adsorption because the accompanying temperatures are high and estimated in a quantity greater than ((40 kj/mol), and this type of adsorption is specific and is not reversed and limited by its layer Oxygen adsorption on coal surface [39].

12. Time effect

The effect of time was referring to extraction iron complex by solid phase. It was studied shacking time by shaker from 5 min to 30 min was shown in (Fig. 13) under optimum at pH 7, concentration salicylaldehyde oxime reagent 0.04 mol. L^{-1} and amount sorbent 0.1 gm and temperature 308 K. The best time to separation iron (III) ligand complex from solid phase (silica) at 15 min.

13. Ferric ion extraction application

A series of drugs containing iron were used at the forms of ampoules or tablets [40] such as (Hemafer, Ferblex, Ferimax, Akourose and Sorbifer Duroles) as the applications of Ferric Ion Extraction on solid phase (silica). Which it was used concentration of the drugs at 25 mg. L^{-1} by using conditions experimental (at temperature of 35 °C, pH 7, amount of solid phase 0.1 gm and adsorption time 15 min. However, before and after adsorption of the drugs as shown in Table 3. The silica was most surface to extraction iron from different types of drugs. Silica have chemical properties to adsorb iron compounds in drugs. It was the polarity of the silica surface to improving extraction percentage. The interaction between silica and the iron compounds allows for better separation in the drugs [41,42].

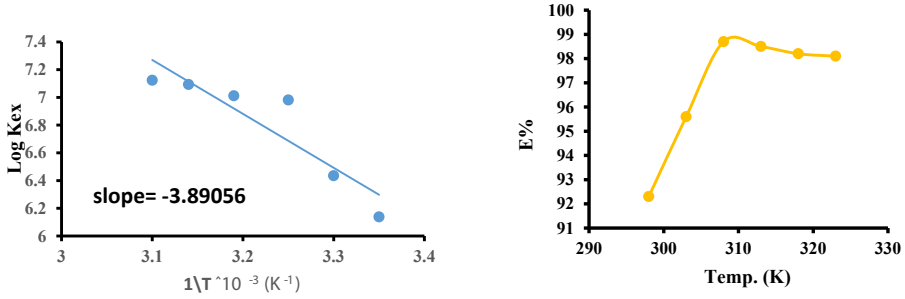

Fig. 12. Effect of temperature on Fe^{+3} complex adsorption on to silica.

Table 3. Adsorption the silica in to ferric ion in different types of drugs.

Name Of Drug	Dos of drug	Mean ± SD before ads	Mean ± SD after ads	D	E %
Hemafer	100 mg\5 ml	0.072 ± 0.00264	0.008 ± 0.00251	9.0	90.0
Ferblex	40 mg\15 ml	0.088 ± 0.00757	0.024 ± 0.00264	3.7	78.7
Ferimax	100 mg\2 ml	0.071 ± 0.00300	0.022 ± 0.00458	3.2	76.2
Akourose	100 mg\5 ml	0.078 ± 0.00251	0.012 ± 0.00153	6.5	86.7
Sorbifer Duroles	100 mg\60 mg	0.148 ± 0.00251	0.027 ± 0.00472	5.5	84.6

14. Conclusion

Mesoporous silica was successfully synthesized from soil from Karbala city in Iraq using the sol-gel method. Characterization results from various analytical techniques confirm the composition and quality of the mesoporous structure: EDS analysis confirmed the high purity of the silica, with silicon and oxygen percentages by weight ranging from 31.8 to 50.8. XRD analysis indicated an amorphous silica structure. Scanning electron microscope (SEM) images revealed the mesoporous morphology and particle distribution. FTIR spectra showed characteristic absorption of Si-O-Si stretching and vibrations. BET texture analysis revealed a high specific surface area of 252.71 and a pore diameter of 11.20, indicating the mesoporous range. Mesoporous silica proved to be an effective that highly purity and permeability for adsorbent, with medium concentrations, temperatures, and high extraction percent of iron (III) complexes from aqueous solutions by dispersive solid phase extraction method demonstrating the effectiveness and precision of this method and its successful application to pharmaceutical samples.

Ethical Approval

This research is a study of the properties of the material used in dental fillings. It has not been applied to humans.

Data Availability

All data is in the search.

Author Contributions

All authors contributed equally to this work. Each author participated in the conceptualization, methodology, data analysis, and manuscript preparation.

Source of Funding

No funding.

Conflict of Interest

No conflicts of interest.

Acknowledgments

We would like to extend my sincere thanks to Kerbala University, the College of Science, and the Department of chemistry for their continuous support in completing this research.

References

[1] Rizzi F, Castaldo R, Latronico T, Lasala P, Gentile G, Lavorgna M, et al. High surface area mesoporous silica nanoparticles with tunable size in the sub-micrometer regime: insights on the size and porosity control mechanisms. Molecules 2021;26(14):4247.
[2] Olivieri F, Castaldo R, Cocca M, Gentile G, Lavorgna M. Mesoporous silica nanoparticles as carriers of active agents for smart anticorrosive organic coatings: a critical review. Nanoscale 2021;13(20):9091–111.
[3] Rahim O, Achoura D, Benzerara M, Bascoulès-Perlot C. Experimental contribution to the study of the physic-mechanical behavior and durability of high-performance concretes based on ternary binder (cement, silica fume and granulated blast furnace slag). Frat Ed Integrità Strutt 2022; 16(59):344–58.
[4] Morais RP, Hochheim S, de Oliveira CC, Riegel-Vidotti IC, Marino CE. Skin interaction, permeation, and toxicity of silica nanoparticles: challenges and recent therapeutic and cosmetic advances. Int J Pharm 2022;614:121439.
[5] Zhao H, Guo M, Li F, Zhou Y, Zhu G, Liu Y, et al. Fabrication of gallic acid electrochemical sensor based on interconnected Super-P carbon black@ mesoporous silica nanocomposite modified glassy carbon electrode. J Mater Res Technol 2023;24:2100–12.
[6] Meier M, Ungerer J, Klinge M, Nirschl H. Synthesis of nanometric silica particles via a modified Stöber synthesis route. Colloids Surf A Physicochem Eng Asp 2018;538: 559–64.
[7] Chun J, Lee JH. Recent progress on the development of engineered silica particles derived from rice husk. Sustainability 2020;12(24):10683.
[8] Innocenzi P. Sol-gel processing for advanced ceramics, a perspective. Open Ceramics 2023:100477.
[9] Navas D, Fuentes S, Castro-Alvarez A, Chavez-Angel E. Review on sol-gel synthesis of perovskite and oxide nanomaterials. Gels 2021;7(4):275.
[10] Lei Q, Guo J, Noureddine A, Wang A, Wuttke S, Brinker CJ, et al. Sol–gel-based advanced porous silica materials for biomedical applications. Adv Funct Mater 2020;30(41): 1909539.
[11] Ali HH, Mihsen HH, Hussain KA. Synthesis, characterization and antimicrobial studies of modified silica materials derived from rice husks. BioNanoScience 2023;13(3): 1163–76.
[12] Hoang CV, Thoai DN, Cam NTD, Phuong TTT, Lieu NT, Hien T, et al. Large-scale synthesis of nanosilica from silica

sand for plant stimulant applications. ACS Omega 2022;7 (45):41687–95.
[13] Shojaei S, Nouri A, Baharinikoo L, Farahani MD, Shojaei S. Removal of the hazardous dyes through adsorption over nanozeolite-X: simultaneous model, design and analysis of experiments. Polyhedron 2021;196:114995.
[14] Shojaei S, Shojaei S, Band SS, Farizhandi AAK, Ghoroqi M, Mosavi A. Application of Taguchi method and response surface methodology into the removal of malachite green and auramine-O by NaX nanozeolites. Sci Rep 2021;11(1):16054.
[15] Jiang N, Chang X, Zheng H, He Q, Hu Z. Selective solid-phase extraction of nickel (II) using a surface-imprinted silica gel sorbent. Anal Chim Acta 2006;577(2):225–31.
[16] Płotka-Wasylka J, Jatkowska N, Paszkiewicz M, Caban M, Fares MY, Dogan A, et al. Miniaturized solid phase extraction techniques for different kind of pollutants analysis: state of the art and future perspectives–PART 2. TrAC, Trends Anal Chem 2023;165:117140.
[17] Shojaei S, Shojaei S, Nouri A, Baharinikoo L. Application of chemometrics for modeling and optimization of ultrasound-assisted dispersive liquid–liquid microextraction for the simultaneous determination of dyes. NPJ Clean Water 2021; 4(1):23.
[18] Szynkiewicz D, Georgiev P, Ulenberg S, Bączek T, Belka M. Dispersive solid-phase extraction facilitated by newly developed, fully 3D-printed device. Microchem J 2023;187: 108367.
[19] Belarbi S, Vivier M, Zaghouani W, De Sloovere A, Agasse V, Cardinael P. Comparison of different d-SPE sorbent performances based on quick, easy, cheap, effective, rugged, and safe (QuEChERS) methodology for multiresidue pesticide analyses in rapeseeds. Molecules 2021;26(21):6727.
[20] Meftah N, Hani A, Merdas A. Extraction and physico-chemical characterization of highly-pure amorphous silica nanoparticles from locally available dunes sand. Chem Afr 2023;6(6):3039–48.
[21] Tonković M, Hadžija O. Use of salicylaldehyde for the spectrophotometric determination of Fe(III). Microchim Acta 1985;87(1):133–8.
[22] Khudhair AF, Hassan MK. Cloud point extraction and determination trace iron (III) in urine samples by spectrophotometry and flame atomic absorption spectrometry. Asian J Chem 2017;29(12):2725–33.
[23] Meftah N, Hani A, Merdas A, Sadik C, Sdiri A. A holistic approach towards characterizing the El-Oued siliceous sand (eastern Algeria) for potential industrial applications. Arabian J Geosci 2021;14:1–14.
[24] Didik LA, Damayanti I, Jumliati J, Lestari PA. Morphological characteristics and mineral content analysis of magnetic minerals based on river and coastal sand using SEM-EDX. Jurnal Sains Dasar 2021;10(2):44–50.
[25] Al Khudhair A, Bouchmella K, Mutin PH, Hulea V, Gimello O, Mehdi A. Hydrolytic vs. nonhydrolytic sol-gel in preparation of mixed oxide silica–alumina catalysts for esterification. Molecules 2022;27(8):2534.
[26] Lee S-M, Lee S-H, Roh J-S. Analysis of activation process of carbon black based on structural parameters obtained by XRD analysis. Crystals 2021;11(2):153.
[27] Joni I, Rukiah R, Panatarani C. Synthesis of silica particles by precipitation method of sodium silicate: effect of temperature, pH and mixing technique. In: AIP conference proceedings. AIP Publishing; 2020.
[28] Sattar M. The feasibility of extraction of silicon from sand by metal-thermite reduction process. London Journal of Research of Engineering Research; 2020.
[29] Ndung'u S, Nthiga EW, Wanjau R. Facile extraction and characterization of silica nanopowder from marine national park beach sand via alkali fusion route. 2023.
[30] Sharafudeen R, Al-Hashim JM, Al-Harbi MO, Al-Ajwad AI, Al-Waheed AA. Preparation and characterization of precipitated silica using sodium silicate prepared from Saudi Arabian desert sand. Silicon 2017;9:917–22.
[31] Eddy DR, Ishmah SN, Permana MD, Firdaus ML. Synthesis of titanium dioxide/silicon dioxide from beach sand as photocatalyst for Cr and Pb remediation. Catalysts 2020;10 (11):1248.
[32] Sui D-P, Chen H-X, Li D-W. Sol–gel-derived thiocyanato-functionalized silica gel sorbents for adsorption of Fe (III) ions from aqueous solution: kinetics, isotherms and thermodynamics. J Sol Gel Sci Technol 2016;80:504–13.
[33] Ellerbrock R, Stein M, Schaller J. Comparing amorphous silica, short-range-ordered silicates and silicic acid species by FTIR. Sci Rep 2022;12(1):11708.
[34] Nelson ES, Iyuke S, Daramola MO, Okewale A. Extraction and characterization of silica from empty palm fruit bunch (EPFB) Ash. Processes 2023;11(6):1684.
[35] Lazaar K, Pullar R, Hajjaji W, Mefteh S, Medhioub M, Jamoussi F. Preparation of silica gel obtained from early cretaceous Sidi Aich sands (Central Tunisia). 2021.
[36] Boualem A, Leontie L, Lopera SAG, Hamzaoui S. Synthesis and characterization of mesoporous silica from Algerian river sand for solar grade silicon: effect of alkaline concentration on the porosity and purity of silica powder. Silicon 2022;14(10):5231–40.
[37] Rosenberg DJ, Alayoglu S, Kostecki R, Ahmed M. Synthesis of microporous silica nanoparticles to study water phase transitions by vibrational spectroscopy. Nanoscale Adv 2019;1(12):4878–87.
[38] Mladin G, Ciopec M, Negrea A, Duteanu N, Negrea P, Ianasi P, et al. Silica-iron oxide nanocomposite enhanced with porogen agent used for arsenic removal. Materials 2022;15(15):5366.
[39] Aljamali NM, Khdur R, Alfatlawi IO. Physical and chemical adsorption and its applications. Int J Therm Chem Kinet 2021;7(2):1–8.
[40] Hamran BN, Khudhair AF. Micellar determination of amoxicillin in the pharmaceutical compounds by using cloud point extraction. Res J Pharm Technol 2020;13(2): 732–41.
[41] Giret S, Wong Chi Man M, Carcel C. Mesoporous-silica-functionalized nanoparticles for drug delivery. Chem-Eur J 2015;21(40):13850–65.
[42] Zinoveev D, Pasechnik L, Fedotov M, Dyubanov V, Grudinsky P, Alpatov A. Extraction of valuable elements from red mud with a focus on using liquid media—a review. Recycling 2021;6(2):38.